

# ATMOSPHERIC PRE-CORRECTED DIFFERENTIAL ABSORPTION TECHNIQUES TO RETRIEVE COLUMNAR WATER VAPOR: APPLICATION TO AVIRIS 91/95 DATA

Daniel Schl pfer<sup>1</sup>, Christoph C. Borel<sup>2</sup>, Johannes Keller<sup>3</sup> and Klaus I. Itten<sup>4</sup>

<sup>1</sup> permanent address: Department of Geography, RSL, University of Z rich, CH-8057 Z rich, Switzerland  
Phone: +41 1 257 52 49, Fax: +41 1 362 52 27, E-mail: dschlappf@rsl.geogr.unizh.ch

<sup>2</sup> Los Alamos National Laboratory, NIS-2, MS C323, Los Alamos, NM 87545, USA

<sup>3</sup> Paul Scherrer Institut (PSI), CH-5232 Villigen PSI, Switzerland

<sup>4</sup> Remote Sensing Laboratories (RSL), Department of Geography, University of Z rich, CH-8057 Z rich, Switzerland

## 1 INTRODUCTION

Water vapor is one of the main forces for weather development as well as for mesoscale air transport processes. The monitoring of water vapor is therefore an important aim in remote sensing of the atmosphere. Current operational systems for water vapor detection use primarily the emission in the thermal infrared (AVHRR, GOES, ATSR, Meteosat) or in the microwave radiation bands (DMSP). The disadvantage of current satellite systems is either a coarse spatial (horizontal) resolution ranging from one to tens of kilometers or a limited insight into the lower atmosphere. Imaging spectrometry on the other hand measures total column water vapor contents at a high spatial horizontal resolution and has therefore the potential of filling these gaps.

The sensors of the AVIRIS instrument are capable of acquiring hyperspectral data in 224 bands located in the visible and near infrared at 10 nm resolution. This data includes the information on constituents of the earth's surface as well as of the atmosphere. The optical measurement of water vapor can be performed using sensor channels located in bands or lines of the absorption spectrum. The AVIRIS sensor has been used to retrieve water vapor and with less accuracy carbon dioxide, oxygen and ozone. To retrieve the water vapor amount, the so called differential absorption technique has been applied (Carr re et al., 1993; Kaufman et al., 1992). The goal of this technique is to eliminate background factors by taking a ratio between channels within the absorption band and others besides the band. Various ratioing methods on the basis of different channels and calculation techniques were developed.

The influence of a trace gas of interest on the radiance at the sensor level is usually simulated by using radiative transfer codes. In this study, the spectral transmittance and radiance are calculated by MODTRAN3 simulations with the new DISORT option (Abreu et al., 1995). The objective of this work is to test the best performing differential absorption techniques for imaging spectrometry of tropospheric water vapor.

## 2 ATMOSPHERIC PRE-CORRECTION

The radiance at the sensor level  $L_s$  can be expressed in a simple form as the sum of the ground reflected radiance  $L_{gnd}$  (including direct and path scattered ground reflected radiance) and the backscattered atmospheric radiance  $L_{atm}$  not reflected by the ground:

$$L_s(\rho, h) = L_{gnd}(\rho, h) + L_{atm}(h) \quad (1)$$

The second term is not dependent on the ground reflectance  $\rho$  but is sensitive to the atmospheric composition, in particular the aerosol amount and the water vapor content, which values depend on the ground altitude  $h$ . At low ground reflectance, the atmospheric radiance is the major contributor to the total radiance, whereas at higher reflectance the first term dominates. Erroneous water vapor contents are retrieved, because the second term acts as a ground reflectance independent offset to the first term (Gao and Goetz, 1990a).

For an improved water vapor retrieval it is therefore necessary to perform an atmospheric pre-correction by subtracting an estimate of  $L_{am}(h)$  from the radiometrically calibrated data. The height and channel dependent atmospheric radiance can be estimated by simulating the total radiance at the sensor at zero albedo. It can be shown, that the atmospheric pre-corrected differential absorption method (APDA, see section 3) is insensitive to variations of the ground reflectance, whereas without the atmospheric pre-correction a clear dependency on ground reflectance results. If it is possible to perform a satisfactory atmospheric pre-correction as described, the differential absorption ratio values will only be dependent on an apparent water vapor transmittance. The effects of atmospheric pre-correction, simulated over various surface types and the improvements on water vapor retrieval are shown in detail by Borel and Schl  pfer (1996).

### 3 DIFFERENTIAL ABSORPTION TECHNIQUES

Differential absorption techniques are a practicable way to determine trace gas contents from a spectrum of an absorption band, which is easy to implement at low computing time costs. In general they perform a ratioing between channels within the absorption feature (measurement channels) and channels in its vicinity (reference channels) to detect the relative strength of absorption. Curve fitting techniques (Gao and Goetz, 1990a) are not considered in this study, because of their higher complexity and computing time. Table 1 shows a compilation of the considered techniques.

Method	Abbreviation	# Meas. channels	# Ref. channels	Source	Remarks
Continuum Interpolated Band Ratio	CIBR	1	2	Bruegge, 1990	common water vapor retrieval technique
Linear Regression Ratio	LIRR	$\geq 1$	$\geq 3$	Schl��pfer, 1995	extended CIBR technique
Atmospheric Pre-corrected Differential Absorption technique	APDA	$\geq 1$	$\geq 2$	new	see paper

Table 1: Differential absorption techniques used in this study.

The reflectance slope can be taken into account by using reference channels on both sides of the absorption band. One measurement channel is ratioed to a linear interpolated value at the same wavelength between two reference channels. The quotient of this 'Continuum Interpolated Band Ratio' technique (CIBR, Bruegge et al., 1990) is calculated as:

$$R_{CIBR} = \frac{L_m}{\omega_{r1} \cdot L_{r1} + \omega_{r2} \cdot L_{r2}} \quad \text{where:} \quad \omega_{r1} = \frac{\lambda_{r2} - \lambda_m}{\lambda_{r2} - \lambda_{r1}} \quad \text{and} \quad \omega_{r2} = \frac{\lambda_m - \lambda_{r1}}{\lambda_{r2} - \lambda_{r1}} \quad (2)$$

where  $L_m$  is the radiance at the measurement channel with its central wavelength  $\lambda_m$  and  $L_{r1}, L_{r2}$  are the radiances at the reference channels at the central wavelengths  $\lambda_{r1}, \lambda_{r2}$ . The sensor's noise is one of the big error sources for a precise trace gas measurement, which is reduced by the consideration of a maximum number of selected channels. A linear regression through the reference channels is used to compute a radiance at the center wavelength of the measurement channels. This Linear Regression Ratio (LIRR) is an extension of the CIBR by more suitable channels.

$$R_{LIRR} = \frac{\overline{L_m}}{LIR([\lambda_r], [L_r]) \Big|_{\lambda_m}} \quad \text{and} \quad R_{APDA} = \frac{\overline{L_m - L_{atm,m}}}{LIR([\lambda_r], [L_r - L_{atm,r}]) \Big|_{\lambda_m}} \quad (3a, 3b)$$

where  $\overline{L_m}$  is the mean of the signal in the measurement channels with the corresponding mean wavelength  $\overline{\lambda_m}$ , and  $LIR([x],[y])$  is a linear regression through the defined vectors. When the atmospheric pre-correction is applied by subtracting the atmospheric not ground reflected radiance from the radiance at the sensor, the LIRR becomes an atmospheric pre-corrected differential absorption technique (APDA, equation 3b). For one measurement channel and two reference channels the equation 3a reduces to the CIBR calculation (eq. 2) and equation 3b reduces to the 3-channel APDA technique, described in Borel and Schl pfer (1996).

## 4 EVALUATION OF DIFFERENTIAL ABSORPTION TECHNIQUES

### 4.1. CHANNEL SELECTION

The two channel categories mentioned in section 2 are evaluated using the channel selection procedure proposed by Schl pfer et al. (1995a). Measurement channels are searched within the absorption band because they should be sensitive to variations of the trace gas amount. Furthermore the difference between the signal of the trace gas and the noise must be clearly discernible in these channels and other absorbing atmospheric species must not disturb the signal of the trace gas of interest. A reference channel has to meet two conditions: The signal should not be influenced by any atmospheric species and the effective signal to noise ratio must be as big as possible. The mentioned requirements were expressed as mathematical channel qualifiers for measurement and reference channels by Schl pfer et al. (1995a). One factor, which has to be considered in addition to the mathematical selection procedure is the wavelength distance of the reference channels from their corresponding measurement channels. It has to be minimized to reduce errors due to non-linearity effects of the background radiance.

The channel selection procedure was applied to simulated data corresponding to AVIRIS images from 1991 over Central Switzerland and from 1995 over Camarillo (California). Ranked sets of channels to be used in differential absorption techniques were defined. First analysis showed, that the best suited wavelength region is the 940 nm absorption band. Hence, only channels in its region (from about 850 nm to 1070 nm) were further considered (see table 2). A crucial factor for the channel selection is the total water vapor transmittance, which has to be estimated from an average total columnar water vapor content for each scene. In 1995 the average transmittance was not exactly known from radiosonde data. Therefore the best channels on both sides of the maximal absorption (channels 59 and 64; both in the slope of the absorption feature) were also selected for further evaluations.

	AVIRIS 1991 data	AVIRIS 1995 data
measurement channels	60 (939 nm; $\sigma$ -band) 61 (949 nm; $\sigma$ - $\tau$ -band)	59 (912 nm; $\rho$ -band) 61 to 64 (932 - 961 nm; $\sigma$ - $\tau$ -band)
reference channels (near the selected meas. channels)	52 to 54 (862 - 881 nm) 66 to 73 (987 - 1065 nm)	54 to 56 (865 - 884 nm) 68 to 70 (999 - 1018 nm)

Table 2: The best performing measurement and reference channels for water vapor measurement, based on the characteristics of 1991 and 1995 AVIRIS data.

### 4.2 METHOD SELECTION

A good method for the measurement of a trace gas must meet the following requirements: 1) little noise effects due to the statistic error of the single channels, 2) low cross sensitivity to variations of disturbing atmospheric constituents, and 3) insensitivity to changing ground reflectance characteristics. The techniques given in section 3 are applied for various channel combinations and tested regarding the above conditions. Each of the latter is described by a metric value.

For 1991 data a large set of methods was compared by multiplying these values (similar to the channel selection procedure) and by setting single limits for each metric (Schläpfer et al., 1995b). It was found, that the use of more than 3 channels of the best ranked ones reduces the total image noise without losing information. Techniques of higher complexity like absorption slope analysis or nonlinear regressions failed due their high sensitivity to the sensor noise. The APDA(60,61;53,54,66,67,68) method was finally selected for application to the images (Schläpfer et al., 1995b).

For 1995 data a total number of 360 methods was introduced, consisting of APDA and LIRR/CIBR combinations with 4 (respective 2) reference channels and 2 (respective 1) measurement channels. For the test of atmospheric cross sensitivity, MODTRAN3 runs with varying aerosol and water vapor contents were taken as calibration data for the defined methods. All retrieval methods were then applied to radiance data of a spatial image subset. Since it can be assumed, that the water vapor variability over a small flat area is modest, the standard deviation of the processed water vapor ratio values in this image subset is taken as a measure for errors due to the total image noise (= sensor noise + ground reflectance variations).

A limit for the qualifiers was set to get a pre-evaluated set of methods, which had to fulfill the requirements in the best 10 percent of all 360 methods. The percent limit was interactively reduced until less than 10 methods remained. These methods were applied to images and the columnar water vapor content was quantified. Special effects in the water vapor image, like erroneous channels or obvious misquantifications, led to further exclusions and re-evaluation of other methods. The whole method selection process was performed in two major steps after the channel selection: the theoretical pre-evaluation based on simulations, sensor characteristics and image subsets and a practical evaluation, based on effective quantification results, ground truth comparisons and effects in the resulting image.

As expected, the APDA - technique increased the significance of the water vapor signal against the standard deviation in the 100x100 pixel subset, i. e. the background reflectance influences were suppressed. Also the aerosol influence could be slightly reduced by the atmospheric pre-correction. The error induced by aerosols is nearly twice as big for methods with measurement channels in the slope of the band than for those in the center. Therefore the measurement channels in the absorption maximum had to be used, although those in the slope showed better ranking results after the channel selection procedure.

Figure 1 shows six of the best performing methods for 1995 data. The absolute error was obtained by comparing a relatively small water vapor signal with the two error factors 'Aerosols' and 'Total image noise'. The ratioing to the estimated total water vapor amount of about 29.2 kg/m<sup>2</sup> at image base level yielded the percentage of the relative errors. The estimated errors due to an aerosol variation between visibilities of 23 km and 12 km at ground level was between 1.0 and 1.3 kg/m<sup>2</sup>; corresponding to a relative error of about 3.5 to 4.5% (see figure 1). The combined background reflectance and sensor noise error, given by the standard deviation within the image subset, is nearly half as big with 2 to 2.5% on the retrieved water vapor amount (this error will increase for larger subsets). The channel combination was defined based on the best performing methods as shown in figure 1. The theoretical total error of the retrieval is estimated to be below 5% (aerosol error + image noise error) on the total water vapor amount out of the above method evaluation, which corresponds to a columnar amount of about  $\pm 1.5$  kg/m<sup>2</sup>.

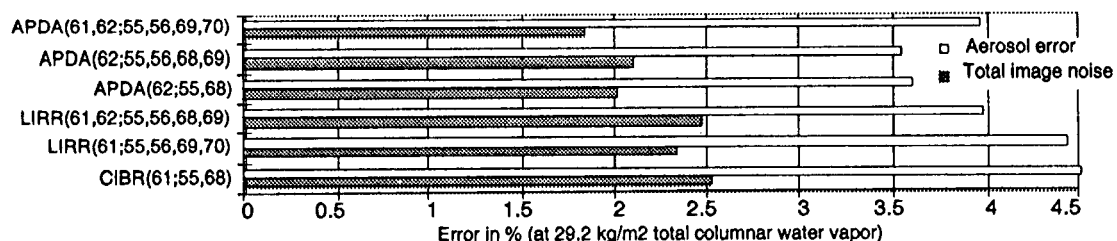


Figure 1: Evaluation results for 1995 AVIRIS data, the water vapor retrieval error is given relative to normal midlatitude summer conditions.

### 4.3 RELATING RATIO VALUES TO TOTAL COLUMNAR WATER VAPOR

The Differential Absorption technique yields only unquantified ratio values, which have to be transformed to total water vapor amounts. Frouin et al. (1989) and Carrere et al. (1993) used an exponential approach for the relationship of a differential absorption ratio  $R$  to its corresponding water vapor amount ( $PW$ ). For this study it was extended to the equation:

$$R = e^{-(\gamma + \alpha(PW)^\beta)} \quad \text{solved for the water vapor amount:} \quad PW = -\left(\frac{\ln(R) + \gamma}{\alpha}\right)^{\frac{1}{\beta}} \quad (4)$$

The water vapor retrieval procedure for image data follows the following steps: First simulated data in the AVIRIS-channels at various total columnar water vapor contents is obtained by MODTRAN3 runs. Then the previously selected, best performing differential absorption technique is applied to the thus simulated radiance at the sensor, what yields a look up table for the relationship between water vapor content and ratio value. The constants  $\alpha$ ,  $\beta$  and  $\gamma$  of the exponential fitting function (4) are derived from the LUT and used to invert the ratio image to the final retrieved total columnar water vapor distribution image. Typical values for  $\alpha$  are 0.12- 0.18, for  $\beta$  0.65 to 0.80 and for  $\gamma$  -0.05 to 0.4. The procedure can be extended by iterative APDA calculations and by using cubic spline interpolations instead of equation (4) (Borel and Schl pfer, 1996).

## 5 APPLICATION TO AVIRIS IMAGES

The methodology described in the previous sections was applied to two AVIRIS scenes:

- 1) Site: Central Switzerland, 'Risch'      Date: July 5, 1991      run 6, scene1
- 2) Site: Santa Monica, 'Camarillo'      Date: May 26, 1995      run 8, scene3

### 5.1 SCENE OVER CENTRAL SWITZERLAND

The selected differential absorption method for 1991 was applied to the AVIRIS'91 scene of Central Switzerland (Meyer, 1994). The '91 data has a five time worse SNR compared with the most recent AVIRIS data. However, this data set is valuable for atmospheric imaging spectrometry because of the extensive simultaneous in-situ measurements of atmospheric trace gases, taken during the Swiss POLLUMET experiment. Various balloon soundings in and near the test region were combined to obtain the actual profile for the date of over flight (5th of July, 1991). The error of these radiosonde measurements is estimated to be within  $\pm 10\%$ . Additionally, the spatial distribution of water vapor was measured by in situ flights of an ultra light aircraft.

The above explained correction of the path radiance effect had to be done to diminish the impact of the background albedo. Since the path radiance is dependent on the ground altitude, a height dependent correction had to be applied. The radiance over zero albedo was simulated at different altitudes using MODTRAN3 with the DISORT option. The height information from the corresponding DEM was used to get a height dependent path radiance for each channel and pixel. This term was then subtracted from the radiometric calibrated 1991 AVIRIS-data and the ratio applied to these corrected data.

The water vapor retrieval results of the APDA(60,61;53,54,66,67,68) method are shown in figure 2. The highest concentrations measured near the lake in the image are about  $29 \text{ kg/m}^2$  and the mean column near the shore is  $28.5 \text{ kg/m}^2$ . The integration of the measured water vapor profiles taken from radiosonde data yields a total column of  $29.7 \text{ kg/m}^2$  over the lake level (414 m a.s.l.). This small difference of about 5% between radiosonde data and the quantified AVIRIS values is within the error of radiosonde data in general and also within the error range of the retrieval procedure described above.

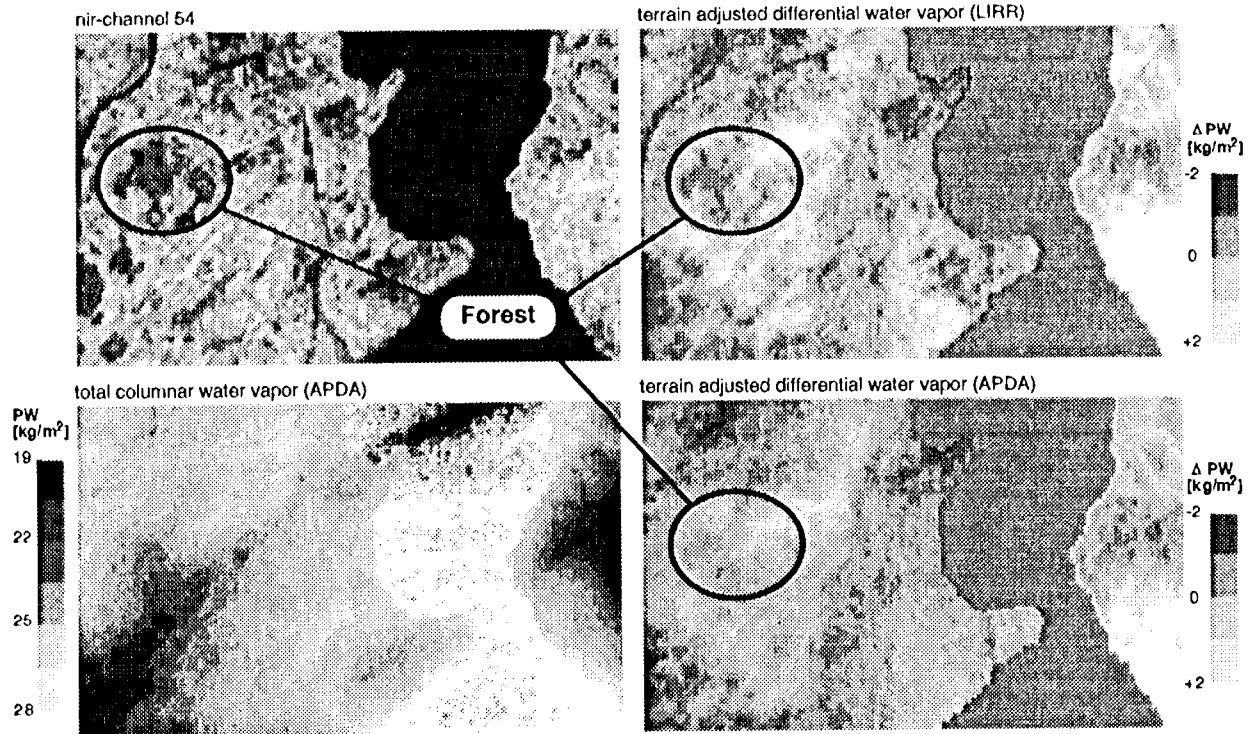


Figure 2: Upper left: raw image (at channel 54, 881 nm); lower left: water vapor retrieval with atmospheric pre-correction; upper right: terrain adjusted differential water vapor distribution without atmospheric pre-correction; lower right: same processing as upper right after height dependent atmospheric pre-correction. All images are smoothed with a filter size of 5x5 pixels. The lake is masked out for the terrain adjusted images.

The spatial water vapor distribution correlates very well with the DTM of the region, because the highest concentrations of water vapor are found in the boundary layer (lower troposphere) with an exponential decrease with height. The difference in terrain height of 540 m produces a decrease of water vapor of about 9 kg/m<sup>2</sup>, which is obtained out of the image between the highest and the lowest terrain point (954 m a.s.l to 414 m a.s.l). The same amount is obtained by integrating the radiosonde profile between these height levels, within an error of about 5%.

For the interpretation of water vapor distribution in rugged terrain, the influence of the terrain overrides real spatial changes in water vapor concentrations. This effect of the terrain was reduced by calculating an average 'ideal' water vapor distribution map based on the digital elevation model and the average total columnar water vapor contents at each height level. This water vapor distribution averaged at each height level was then subtracted from the quantified total columnar water vapor distribution. The resulting terrain adjusted differential water vapor maps for LIRR and APDA calculation are shown in figure 2. Obvious underestimations over the relatively dark forests can be observed in the uncorrected image, as already described by Gao and Goetz (1990). If the atmospheric pre-correction is applied, most of these errors caused by variations of the background reflectance disappear, leading to a better estimate of relative water vapor concentrations.

## 5.2 SCENE OVER CAMARILLO, CALIFORNIA

For the 1995 data the total aerosol content was not known exactly. Therefore  $I_{atm}$  determined by MODTRAN3 is not an optimal substitute for  $I_{atm,s}$  in  $I_s - I_{atm,s}$  of Eq. 3b. Instead,  $I_s - f \cdot I_{atm,s}$  was used, where  $f$  is determined empirically as the value, which minimizes the standard deviation of the ratio (Eq. 3b) over a subset of the image. This correction factor was used with the APDA technique for the image data as well as for the corresponding

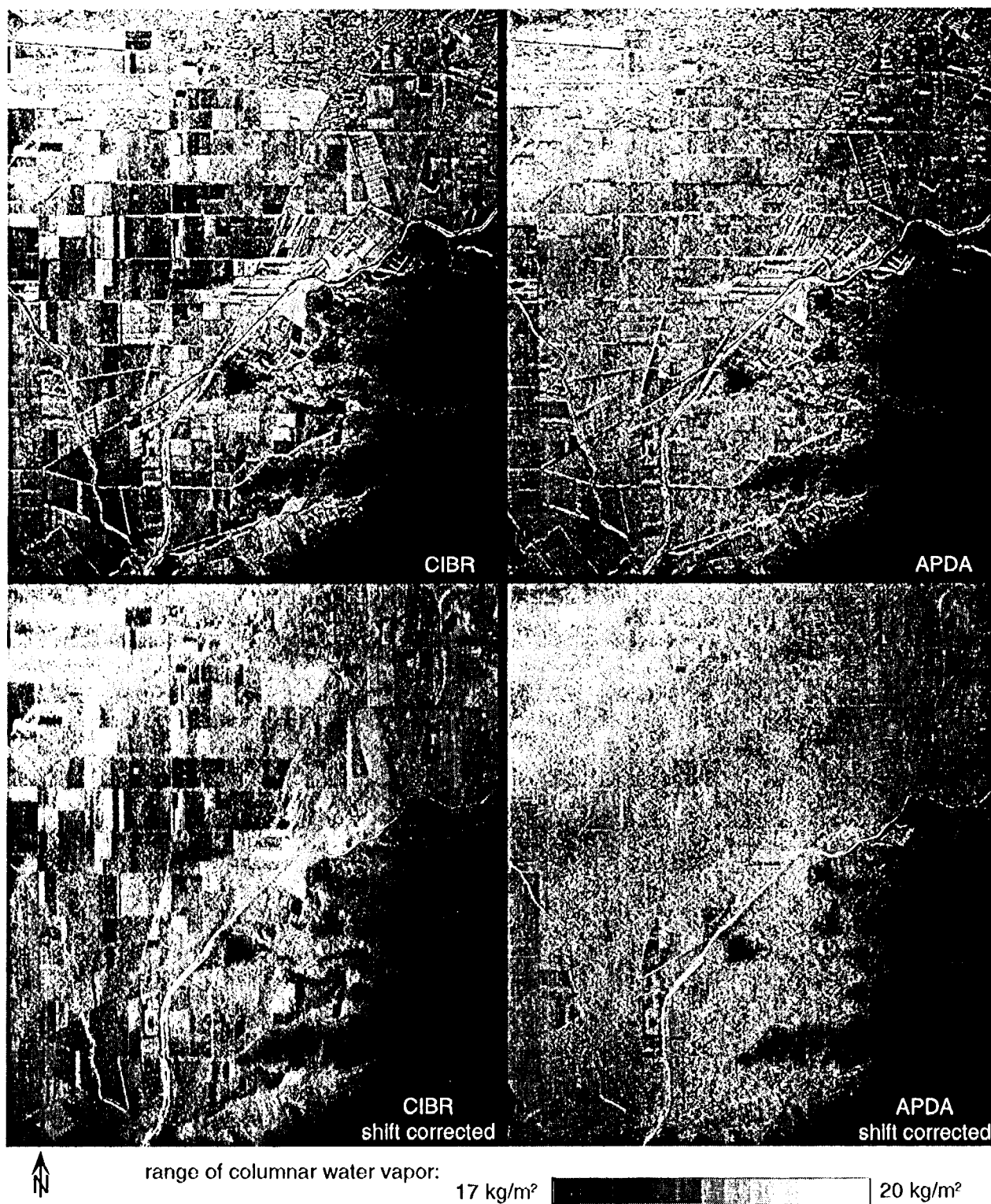


Figure 3: CIBR and APDA(61,62;55,56,68,69) calculation over the 1995 AVIRIS scene at Camarillo (near Oxnard, CA). The images are enhanced to show variations over the plain between Camarillo (northern image border) and Point Mugu (south). The mountain area in the lower right corner appears black, because of the much lower water vapor contents over elevated topography. The four images have not been smoothed.

simulated quantification data. The introduction of that optimization factor is an empirical approach to improve the effect of atmospheric pre-correction, whereas Borel and Schlaepfer (1996) show an iterative approach for the same problem.

The application of the APDA technique on the 1995 data showed the unexpected effects of edge-enhancement along the borders of the agricultural fields (see figure 3, upper images). Since cast shadows in irrigation channels and from plants would not show the observation systematicity, this must be a sensor inherent effect. According to Chrien (1996) the new AVIRIS focal plane features erroneous amplifiers which cause bright areas bounded by dark areas to appear somewhat delayed. The delay increases with the magnitude of changing signal. Since the reference channels have more than twice the signal of the measurement channels, they were delayed. To correct for this effect, a pixel shifting between single channels was assumed (even before we heard about the AVIRIS hardware problem). A procedure to detect sub-pixel shifts (Varosi, 1994) was run over the channels used in the water vapor retrieval algorithm. This analysis, which maximizes the correlation between the single channels, showed that the used reference channels (# 55,56,68,69,70) were shifted across the flight direction by about 0.15 pixels to the measurement channels (# 61,62), whereas in flight direction nearly no shift was detected. All relevant channels were then reregistered by shifting them by the calculated sub-pixel shifts, using bilinear interpolation. The corrected water vapor images were significantly improved compared to the uncorrected images.

Figure 3 shows the effects of atmospheric pre-correction and pixel shift correction: When doing the traditional differential absorption technique, high impacts of the background characteristics are reported (left). After the atmospheric pre-correction most of this impact disappears, but the borders of the fields seem to be enhanced (upper right). Only a pixel shift correction removes this artifact and shows primary water vapor amounts. (The image at the lower right is not smoothed against the others; the smoother appearance is only due to the applied correction steps!).

The range of the water vapor concentrations is within about 17 to 20 kg/m<sup>2</sup>, and even fine variations over the plane between 18 and 19 kg/m<sup>2</sup> can be observed in the shift corrected APDA image. This accuracy can not be achieved with the traditional CIBR-technique, where background effects override the signal of the water vapor. In the final image there are still small ground reflectance caused effects, which show that there is opportunity to improve the water vapor retrieval results by a better atmospheric pre-correction or possibly by using spectral classification techniques.

## 6 CONCLUSIONS

It was shown that the introduced atmospheric pre-corrected differential absorption (APDA) technique allows to measure spatial water vapor distributions even over flat areas with strong background reflectance variations. In advance a quantitative method of channel selection yielded ranged sets of channels for application in the APDA technique, and a large set of retrieval methods were evaluated using an exclusion and ranking process. This combination of optimized channel selection, method evaluation and the APDA technique made it possible to achieve significant improvement compared to traditional differential absorption techniques.

Applying the radiative transfer code MODTRAN3, the selected methods were calibrated to the total water vapor columns. The retrieval of water vapor over land was possible with an accuracy of about  $\pm 5\%$ . The error was attributed to the uncertainty in background reflectance and aerosol concentration in the used atmospheric model. The distribution with terrain height for 1991 data was very similar to the profile measured by radio sondes, although the image was calibrated by the integrated total water vapor column (the slope of the water vapor profile has a negligible effect on the results). Hence, the used methodology has the potential to derive water vapor profiles from the boundary layer, using the digital terrain model.

In future work such profiling methods will be searched and three dimensional modeling of the water vapor field in valleys will be tried. The complementary measurement of water vapor over dark surfaces (like lakes or cast shadow areas) will only be possible with further improvements of the methodology. Such methods will differ essentially from the differential absorption and nonlinear curve fitting techniques. The most promising approaches are the



improvement of the atmospheric pre-correction by introducing an iterative water vapor retrieval process or the application of classification algorithms and spectral databases.

## 7 ACKNOWLEDGMENTS

The following institutions, foundations and persons are greatly acknowledged: The Swiss National Science Foundation and NASA HQ's Remote Sensing Science Program for the financial support of the project, the AVIRIS group at the JPL Pasadena for providing the AVIRIS-images, Los Alamos National Laboratory (LANL) and the Remote Sensing Laboratories (RSL) for their facilities.

## REFERENCES

- ABREU L.W., CHETWYND J.H, ANDERSON G.P. and KIMBALL L.M., 1995: *MODTRAN3 Scientific Report*. draft preprint, Geophysics Laboratory, Air Force Command, US Air Force, Hanscom AFB, MA, USA
- BERK A., BERNSTEIN L.S., ROBERTSON D.C., 1989: *MODTRAN: A Moderate Resolution Model for LOWTRAN 7*. Geophysics Laboratory, Air Force Command, US Air Force, Hanscom AFB, MA, USA
- BRUEGGE C.J., CONEL J.E., MARGOLIS J.S., GREEN R.O., TOON G., CARRÈRE V., HOLM R.G. and HOOVER G., 1990: *In-situ Atmospheric Water-Vapor Retrieval in Support of AVIRIS Validation.*, SPIE Vol. 1298 Imaging Spectroscopy of the Terrestrial Environment, pp 150 - 163
- BOREL C.C and SCHLÄPFER D., 1996: *Atmospheric Pre-Corrected Differential Absorption Techniques To Retrieve Columnar Water Vapor: Theory*. Proceedings of the 6th JPL Airborne Earth Science Workshop, JPL, Pasadena (in press)
- CARRÈRE V. and CONEL J. E., 1993: *Recovery of Atmospheric Water Vapor Total Column Abundance from Imaging Spectrometer Data Around 940 nm - Sensitivity Analysis and Application to Airborne Visible/Infrared Imaging Spectrometer (AVIRIS) Data*. Remote Sensing of Environment, Nr. 44 , pp 179 - 204
- CHRIEN T., 1995: *personal communication*, mentioned in xxxx.errata-file of AVIRIS data set
- FROUIN R., DESCHAMPS P.-Y and LECOMTE P., 1990: *Determination from Space of Atmospheric Total Water Vapor Amounts by Differential Absorption near 940 nm: Theory and Airborne Verification*. Journal of Applied Meteorology, Vol. 29, American Meteorological Society, pp 448 - 459
- GAO B.-C., Heidebrecht K.B and GOETZ A.F.H., 1993: *Derivation of Scaled Surface Reflectance from AVIRIS Data*, Remote Sensing of Environment, Nr. 44, New York, pp 165 - 178
- GAO B.-C. AND GOETZ A.F.H., 1990a: *Column Atmospheric Water Vapor and Vegetation Liquid Water Retrievals From Airborne Imaging Spectrometer Data*, Journal of Geophysical Research, Vol. 95, No. D4, pp 3549 - 3564
- GAO B.-C. AND GOETZ A.F.H., 1990b: *Determination of Total Column Water Vapor in the Atmosphere at High Spatial Resolution from AVIRIS Data Using Spectral Curve Fitting and Band Ratioing Techniques*, SPIE Vol. 1298, Imaging Spectroscopy of the Terrestrial Environment, pp 138 - 149
- KAUFMAN Y.J. and GAO B.-C., 1992: *Remote Sensing of Water Vapor in the Near IR from EOS/MODIS*. IEEE Transactions on Geoscience and Remote Sensing, Vol. 30, No. 5, pp 871 - 884
- MEYER P., 1994: *A Parametric Approach for the Geocoding of Airborne Visible/Infrared Spectrometer (Aviris) Data in Rugged Terrain.* , Remote Sensing of Environment, Vol. 48, pp 1-25
- SCHLÄPFER D., KELLER J. and ITTEN K.I., 1995a: *Imaging Spectrometry of Tropospheric Ozone and Water Vapor*. submitted to EARSeL International Journal 'Advances in Remote Sensing', p 12
- SCHLÄPFER D., KELLER J. and ITTEN K.I., 1995b: *Imaging Spectrometry of Tropospheric Ozone: New Methods of Channel Selection*, presented at IGARSS'95, Florence, separatum (not in proceedings), p 3
- VAROSI F, 1988-1995: *Varosi's General Purpose IDL Code Library (vlib)* , Mail Code 685, ftp://idlastro.gsfc.nasa.gov /contrib/varosi, NASA/Goddard Space Flight Center, Greenbelt MD
- VERMOTE E., TANRÉ D., DEUZÉ J.L., HERMAN M. and MORCETTE J.J., 1984: *Second Simulation of the Satellite Signal in the Solar Spectrum.* , 6S User Guide Version 0, NASA-Goddard Space Flight Center, Greenbelt, USA, p 182